

PEDOT / PVC-modified Amperometric Carbon Electrodes for Acetylcholine Detection

Peibo Xu†, Hazirah Ismah Muhamad Rapidi †, Sidrah Ahmed†, Daniel Kenneth Abel†, Kiersten Garcia, Ran Chen, Nicholas Toshio Iwai, Mei Shen*

Department of Chemistry, The Beckman Institute for Advanced Science and Technology, University of Illinois at Urbana-Champaign, Urbana, IL 61801, United States

† Equal contribution.

*Corresponding author

E-mail address: mshen233@illinois.edu

Table of Contents

1. Materials and Reagents.

2. Experimental Details.

3. Additional Discussions.

3.1 EDS Study of Bare Carbon and PEDOT-modified Carbon Electrodes.

3.2 Electrochemical Characterization of PEDOT Modification.

3.3 Sensing Mechanism Study.

4. Figures and Table.

Fig. S1 SEM images of PEDOT deposited electrode at (A) 600-times magnification; (B) 18000-times magnification.

Fig. S2 SEM image of carbon-only electrode.

Fig. S3 EDS spectrum of the electrode (A) after electrodeposition of PEDOT; (B) before the PEDOT deposition (carbon-only electrode).

Fig. S4 SEM and EDS results indicate the uniform deposition of PEDOT. (A) SEM image of PEDOT-deposited carbon electrode at 500-times magnification, and (B) corresponding sulfur mapping using EDS.

Fig. S5 Electrochemical characterization of PEDOT-deposited glassy carbon electrodes. (A) Cyclic Voltammograms (CVs) of PEDOT-deposited glassy carbon electrode in ASW (artificial seawater) under different scan rates. (B) A plot of current as a function of scan rate.

Fig. S6 (A) CVs of ACh detection before background subtraction (background-subtracted CVs are shown in Fig. 4). (B) Calibration curve (currents at diffusion-limited potential vs. concentration) for background-subtracted CVs shown in Fig. 4. Diffusion-limited potential used is -0.15 V vs. Ag/AgCl/1M KCl.

Fig. S7 CVs illustrating ACh detection with expanded concentration ranges included. (A) CVs for background (ASW), and 100 nM, 500 nM and 1 μ M ACh added; respectively. (B) CVs for 10 μ M to 100 μ M ACh solution, there is a slight increase in current between 0.2 V to 0 V. (C) CVs for 250 μ M to 1.5 mM ACh solution, there is an obvious increase in current between 0.2 V to 0 V. (D) Background subtracted CVs for 10 μ M to 100 μ M ACh solution, there is an oxidation peak between 0.2 V to 0 V.

Fig. S8 Additional CVs and calibration curves for amperometric ion-selective electrode showing consistency of the results between different researchers, different glassy carbon electrodes, and different supporting electrolytes. (1) Researcher 1 with glassy carbon electrode 1 and TBAPF₆ as the supporting electrolyte. (2) and (3) are repetitive runs by researcher 2 with glassy carbon electrode 3 and TBAPF₆ as the supporting electrolyte. (4) Researcher 3 with TDDATFAB as the supporting electrolyte. For each figure: (A) Raw CVs, (B) background-subtracted CVs, (C) calibration curve at peak current, and (D) calibration curve at diffusion limiting region. The calibration curves showed great linearity between current and ACh concentration irrespective of the differences between electrodes and researchers. These results show high reproducibility for our newly developed amperometry ion-selective ACh electrode.

Fig. S9 CVs on bare carbon electrode before modification. The voltammograms after adding ACh overlaid with that of the background, suggesting that there is no detection of ACh on bare carbon electrode.

Fig. S10 CVs with varying scan rates. (A) CVs for 0.5 mM ACh with different scan rates. (B) Plot of current versus the square root of scan rate. ACh concentration is 0.5mM. (C) CVs for 1.5 mM ACh with different scan rates. (D) Plot of current versus the square root of scan rate. ACh concentration is 1.5 mM. The linear relationship between current and the square root of scan rate suggests the detection of ACh occurs through a solution diffusion process.

Fig. S11 Selectivity study using CVs. CVs after adding interfering species overlapped with that of the background and a significant increase in current was observed after adding ACh, suggesting the selective detection towards ACh against the interfering species. The three repetitive runs for each interfering species showed overlapping responses. Error bar is the standard deviation (n=3).

Fig. S12 Stability of amperometric PVC / PEDOT-modified glassy carbon electrode for the detection of ACh tested 2 months after the fabrication of the acetylcholine (ACh) sensor. (A) Background-subtracted CVs corresponding to ACh detection at varying concentrations. (B) The calibration curve for ACh detection with the current measured at the diffusion-limited region, i.e., 80 mV passing the peak potential.

Fig. S13 Stability test results. The electrode was stored for two months then used to test ACh detection response. (A) Background-subtracted CVs for full potential range. (B) Original CVs before background subtraction. We are still able to see clear detection for ACh, which means the electrode is capable of ACh detection after 2-month storage, showing a great stability of our electrode.

Table S1 EDS results for PEDOT-deposited electrode and carbon-only electrode (before deposition)

1. Materials and Reagents.

Potassium Chloride (KCl) and calcium chloride dihydrate ($\text{CaCl}_2 \bullet 2\text{H}_2\text{O}$) were purchased from VWR (Radnor, PA). Magnesium sulfate anhydrous (MgSO_4), 4-(2-hydroxyethyl)-1-piperazineethanesulfonic acid (HEPES), and acetonitrile were purchased from Fisher Scientific (Hampton, NH). Magnesium chloride hexahydrate ($\text{MgCl}_2 \bullet 6\text{H}_2\text{O}$) and tetrahydrofuran (THF) were purchased from Macron Fine Chemicals distributed by Avantor (Radnor, PA). Sodium chloride (NaCl) was purchased from EMD Millipore (Burlington, MA). Sodium hydroxide (NaOH) was purchased from Ward's Science (Rochester, NY). 3,4-ethylenedioxythiophene (EDOT) was purchased from TCI Chemicals (Tokyo, Japan). Serotonin hydrochloride (5-HT) was purchased from Alfa Aesar (Ward Hill, MA). Tetradodecylammonium chloride (TDDACl), tetrabutylammonium hexafluorophosphate (TBAPF₆), polyvinyl chloride (PVC), o-nitrophenyl octyl ether (NPOE), heptakis (2,6-di-o-methyl)- β -cyclodextrin, γ -aminobutyric acid (GABA), dopamine hydrochloride (DA), L-Ascorbic acid (AA), L-histidine (His), L-lysine (Lys), and acetylcholine chloride (AChCl) were obtained from Sigma-Aldrich (St. Louis, MO). Potassium tetrakis(pentafluorophenyl) borate (TFAB) was from Boulder Scientific Company (Mead, CO). Arginine (Arg) was purchased from Fluka (Buchs, Switzerland). All aqueous solutions were prepared from 18.3 M Ω cm deionized water. Artificial sea water (ASW) is composed of 460 mM NaCl, 10 mM KCl, 10 mM CaCl_2 , 26 mM MgSO_4 , 22 mM MgCl_2 , and 10 mM HEPES. Then the pH of the ASW solution is adjusted to 7.8 using NaOH. The tetrakis(pentafluorophenyl) borate salt (TFAB) of tetradodecylammonium (TDDA) (TDDATFAB) was prepared using metathesis. Aluminum oxide (alumina) powder for polishing electrodes was purchased from Buehler (Lake Bluff, IL).

2. Experimental Details.

2.1 Electrochemical Measurements. The deposition of the poly(3,4-ethylenedioxythiophene)/polyvinyl chloride (PEDOT/PVC) membrane, the detection of acetylcholine (ACh), the study of selectivity, stability, and scan rate dependency of the PEDOT/PVC-modified glassy carbon electrode were accomplished using cyclic voltammetry (CV). All electrochemical measurements for CV and chronoamperometry were performed using a CHI 1205B or CHI 760 potentiostat electrochemical workstation (CHI Instruments, Austin, TX). A three-electrode cell was composed of a commercial silver/silver chloride (Ag/AgCl/1 M KCl) reference electrode (CHI Instruments, Austin, TX), a platinum (Pt) or tungsten (W) wire counter electrode, and a PEDOT/PVC-modified glassy carbon electrode as the working electrode. The Ag/AgCl reference electrode was inserted into a homemade sodium perchlorate/potassium nitrate ($\text{NaClO}_4/\text{KNO}_3$) salt bridge.

2.2 Fabrication and Characterization of the PEDOT / PVC-modified Amperometric Carbon Electrodes. A 3 mm diameter glassy carbon electrode (CHI Instruments, Austin, TX) was cleaned by polishing the surface with 1.0-, 0.3-, and 0.05-micron alumina slurry solutions, followed by sonication in deionized (DI) water for 5 minutes. The 3,4-ethylenedioxythiophene (EDOT) deposition solution was composed of 0.01 M EDOT and 0.1 M TDDATFAB in acetonitrile. Then the PEDOT film was deposited on the polished electrode using this EDOT solution using CV by cycling the potential between -0.3 V to 1.4 V vs Ag/AgCl at 40 mV/s with 22 segments. (An alternative procedure of PEDOT electrodeposition used tetrabutylammonium hexafluorophosphate (TBAPF₆) as the electrolyte to prepare the EDOT deposition solution. The solution was comprised of 0.1 M TBAPF₆ and 0.01 M EDOT in acetonitrile. Then the PEDOT film was deposited on the polished electrode using this EDOT solution using CV by cycling the potential between -0.3 V to 1.4 V vs Ag/AgCl at 40 mV/s with 10 segments) Following the PEDOT deposition, the electrode was immersed in acetonitrile for 45 minutes and rinsed with tetrahydrofuran (THF) for one minute.

A PVC solution made up of 8 mg of PVC, 30 μ L of nitrophenyl octyl ether (NPOE), 4.4 mg of TDDATFAB, and 8.72 mg Heptakis (2,6-di-o-methyl)- β -cyclodextrin in 2 mL of THF was prepared. 5 μ L of the PVC solution was drop-casted on the electrode, which was repeated five times with a five-minute interval in between each drop cast. The electrode was left for 24 hours to dry in the fume hood.

2.3 SEM and EDS Study. The SEM was done using analytical SEM microscope JEOL 7000F. We used 20.0 kV as accelerating voltage. The EDS study was performed on the same SEM microscope with Thermo electron EDS detector. The EDS study for both the PEDOT deposited electrode and glassy carbon electrode were done using 20.0kV accelerating voltage.

2.4 Detection of Acetylcholine. For the detection of ACh, cyclic voltammogram (CV) measurements were taken by cycling the potential between -0.4 V and 0.6 V vs. Ag/AgCl/1M KCl at a scan rate of 100 mV/s. Varying concentrations of 100 nM, 500 nM, 1 μ M, 10 μ M, 30 μ M, 50 μ M, 70 μ M, 100 μ M, 250 μ M, 500 μ M, 750 μ M, 100 μ M, 1250 μ M, and 1500 μ M ACh were added to artificial seawater (ASW), the cellular medium of a common neuronal model. Each of these solutions was tested starting from the background of pure ASW and moving through the ACh concentrations with increasing concentrations. 3 minutes were waited between CV runs.

2.5 Selectivity for Acetylcholine Detection. The selectivity for ACh detection against interfering species was studied by CV measurements. First, the background CV in ASW on the PEDOT / PVC-modified carbon electrode was measured. Then 2.0 mM interfering species were added to ASW in a sequential manner, including ascorbic acid (AA), dopamine (DA), serotonin (5-HT), γ -aminobutyric acid (GABA), and charged amino acids, i.e., histidine (His), arginine (Arg), and lysine (Lys).

2.6 Stability. The PEDOT / PVC-modified glassy carbon electrode was tested for stability over the course of 3 months. After an initial test experiment, the PVC / PEDOT-modified carbon electrode was cleaned and rinsed gently by stirring the electrode in deionized water for three times, then the excess water was removed using a Kimwipe prior to storage. The electrode was stored in the ambient lab environment. After 2-3 months, we repeated the CVs for the detection of ACh on the PEDOT / PVC-modified carbon electrodes using the same procedures presented above.

3. Additional Discussions.

3.1 EDS Study of Bare Carbon and PEDOT-modified Carbon Electrodes. Significantly higher amount of oxygen (O) (8.5%) was measured in PEDOT-modified carbon electrode in comparison to bare carbon electrode (Table S1). Oxygen is another element of PEDOT. In addition, we observed a small amount (0.2%) of aluminium (Al) in PEDOT deposited electrode and a small amount (0.2%) of calcium (Ca) in both PEDOT deposited electrode and the commercial glassy carbon electrode based on the EDS table. The small amount of Al might come from the remaining alumina powder used for polishing. We are not certain about the source of the small amount of Ca observed. The detection limits of EDS were reported to be 0.1%wt¹ or 0.2%-0.5%² depending on the EDS instrument and the material. The amount of Al and Ca we observed is close to the detection limitation of EDS reported by others, thus another possible explanation of this small amount of Al and Ca is error from the EDS characterization.

3.2 Electrochemical Characterization of PEDOT Modification. We characterized the PEDOT-deposited glassy carbon electrode electrochemically in background electrolyte (ASW) using cyclic voltammetry, where different scan rates were employed. The cyclic voltammetry results are shown in Fig.

S5A. It was run at the scan rate of 0.1 V/s at first, and it shows a typical behaviour of double layer charging process as the current remains stable in the potential range between 0.6 V to -0.5 V (vs. Ag/AgCl/1 M KCl). Capacitive current (i_c) can be expressed as $i_c = C \times v$, where C is the capacitance and v is the scan rate. Based on this, capacitive current theoretically increases with scan rate in a linear manner. Thus, we conducted scan rate-dependent experiments to electrochemically characterize PEDOT deposition (Fig. S5, scan rates are shown in Fig.S5). Currents at a potential of 0 V (vs. Ag/AgCl/1 M KCl) were chosen and plotted against the scan rate. The results are shown in Fig. S5B, where currents increase linearly with scan rate with a very good linearity ($R^2 = 0.9998$). This linear response between capacitive currents and scan rates demonstrates that the PEDOT-modified electrode works well as a working electrode as it showed a capacitive current predicted by theory.

3.3 Sensing Mechanism Study. One unknown question is ACh detection mechanism (solution-diffusion vs surface?) of the PVC/PEDOT-Ionophore modified carbon electrodes. We hypothesize that this is a solution-diffusion process. For a solution-diffusion process, Randles–Sevcik equation applies, i.e., $i_p = 0.4463nFAC\sqrt{(NFvD/RT)}$, where the peak current has a linear relationship with the square root of scan rate. Therefore, we performed CV measurements at six different scan rates (0.05, 0.1, 0.3, 0.5, 0.75, 1.0 V/s) at 0.5 mM and 1.5 mM ACh, respectively. Firstly, we measured CVs under these six scan rates in 0.5mM ACh solution. The corresponding CVs are shown in Fig. S10A. Based on the background-subtracted CVs, the detection peak for ACh was found around 0 V (vs. Ag/AgCl/1M KCl). The current at 0V was used as the i_p . Then we plotted the i_p against the square root of scan rate, the result is shown in Fig. S10B, where a very strong linear relationship was observed (R-square is 0.9978). Then we performed the same experiment again in 1.5 mM ACh solution, the CVs of different scan rates are plotted in Fig. S10C and the peak current against the square root of scan rate is plotted in Fig. S10D. For 1.5 mM ACh solution, the linearity between peak current and the square root of scan rate is also very good as R-square is 0.9937. The observed linearity between peak current and the square root of scan rate suggests that amperometric detection of ACh at the PEDOT/PVC-Ionophore modified electrode occurs through a solution-diffusion process.

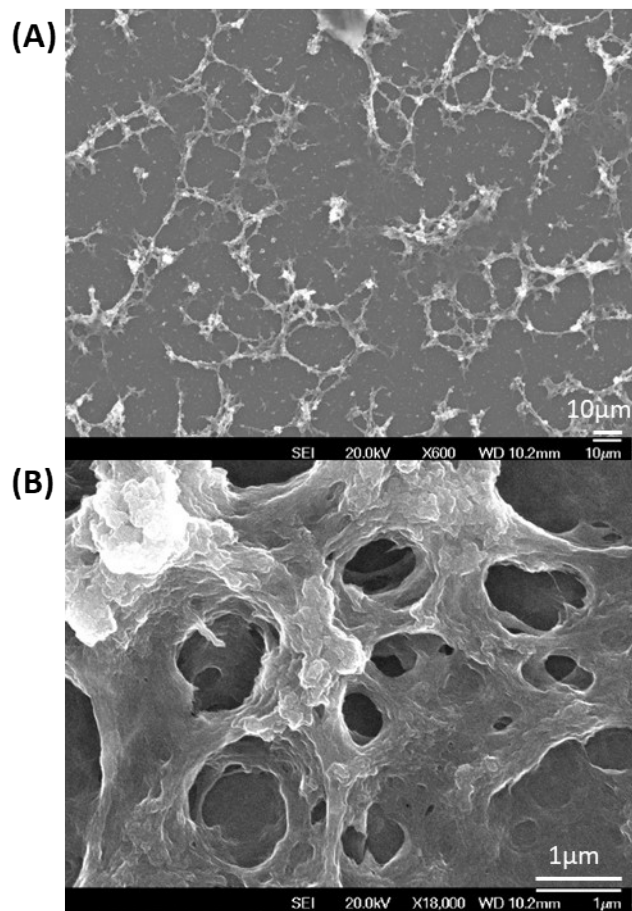


Figure S1. SEM images of PEDOT deposited electrode at (A) 600-times magnification; (B) 18000-times magnification.

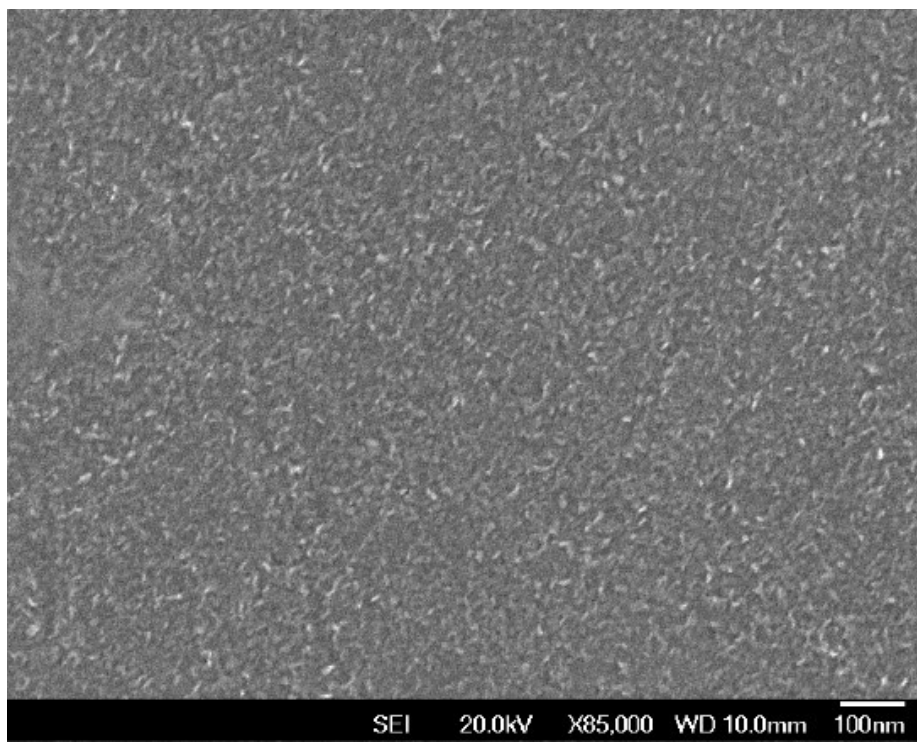


Figure S2. SEM image of carbon-only electrode.

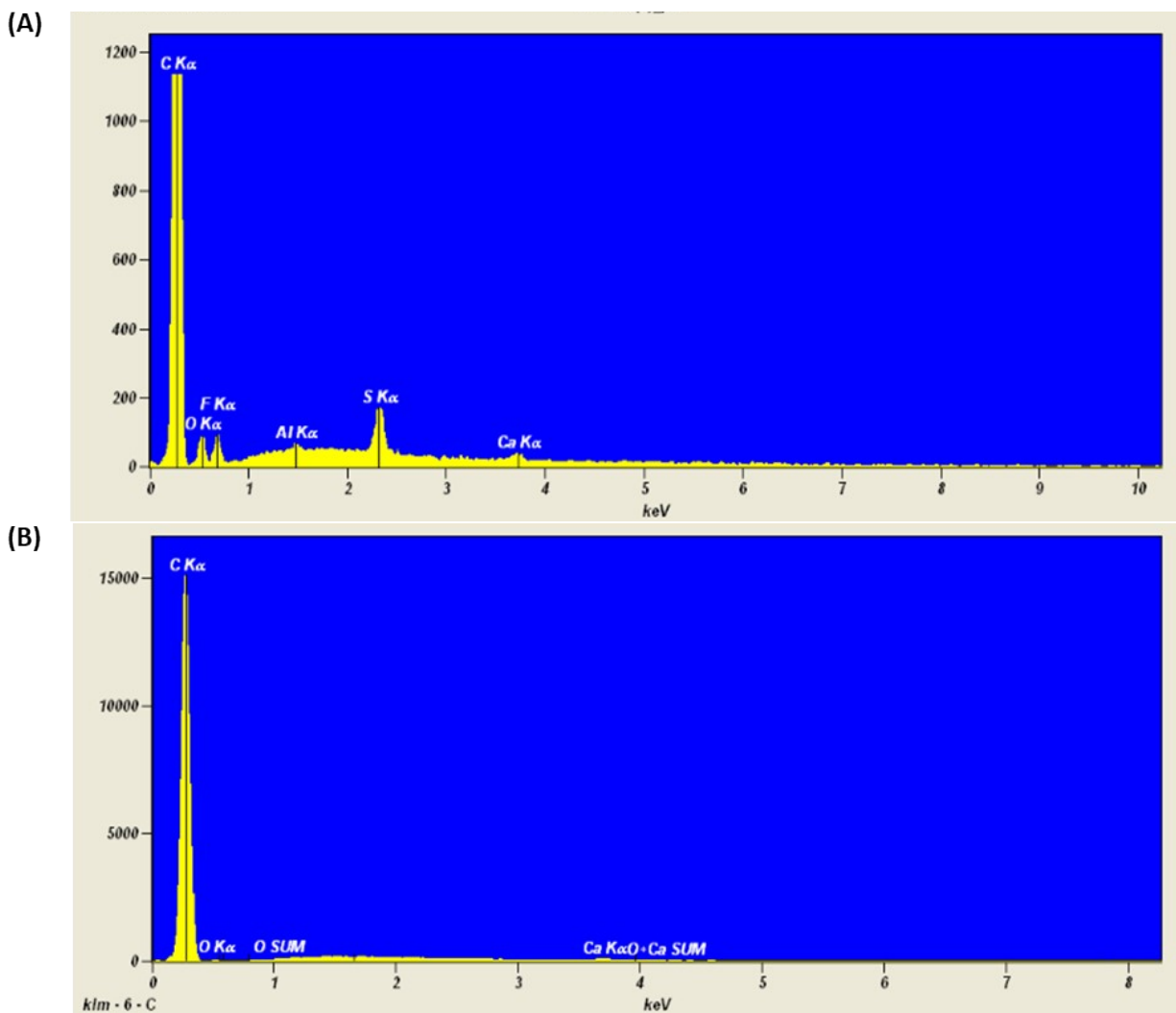


Figure S3. EDS spectrum of the electrode (A) after electrodeposition of PEDOT; (B) before the PEDOT deposition (carbon-only electrode).

Table S1. EDS results for PEDOT-deposited electrode and carbon-only electrode (before deposition).

PEDOT-deposited electrode		Carbon-only electrode (before deposition)	
Element	Atom%	Element	Atom%
C	83.6	C	99.8
Ca	0.2	Ca	0.2
O	8.5	O	Too little to be calculated by software
F	6.2	F	Not detected
S	1.3	S	Not detected
Al	0.2	Al	Not detected

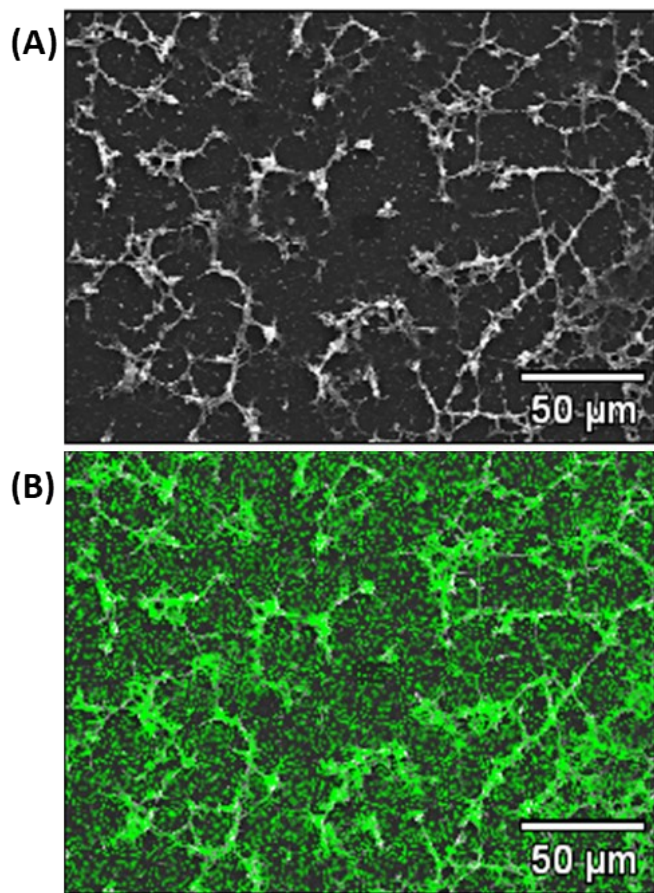


Figure S4. SEM and EDS results indicate the uniform deposition of PEDOT. (A) SEM image of PEDOT-deposited carbon electrode at 500-times magnification, and (B) corresponding sulfur mapping using EDS.

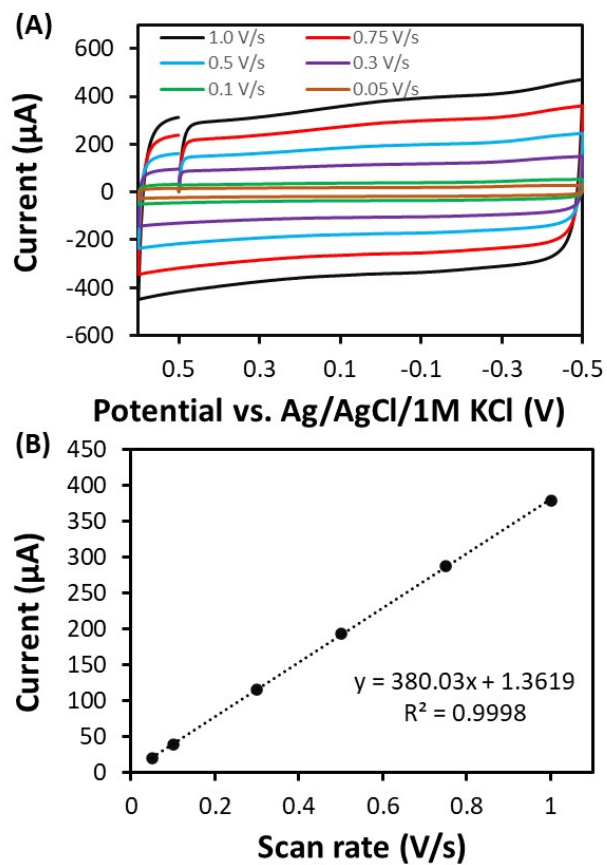


Figure S5. Electrochemical characterization of PEDOT-deposited glass carbon electrodes. (A) Cyclic Voltammograms (CVs) of PEDOT-deposited glassy carbon electrode in ASW (artificial seawater) under different scan rates. (B) A plot of current as a function of scan rate.

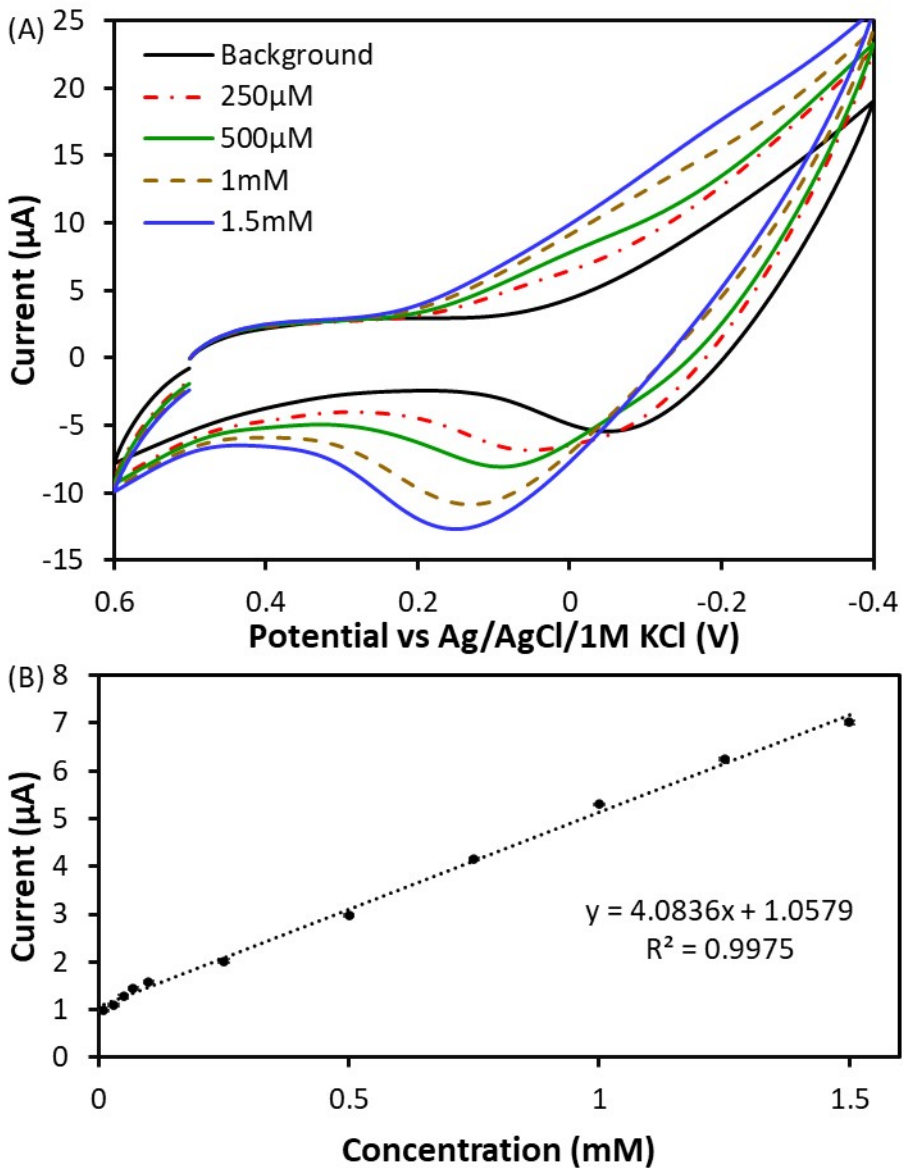


Figure S6. (A) CVs of ACh detection before background subtraction (background-subtracted CVs are shown in Fig. 4). (B) Calibration curve (currents at diffusion-limited potential vs. concentration) for background-subtracted CVs shown in Fig. 4. Diffusion-limited potential used is -0.15 V vs. Ag/AgCl/1M KCl.

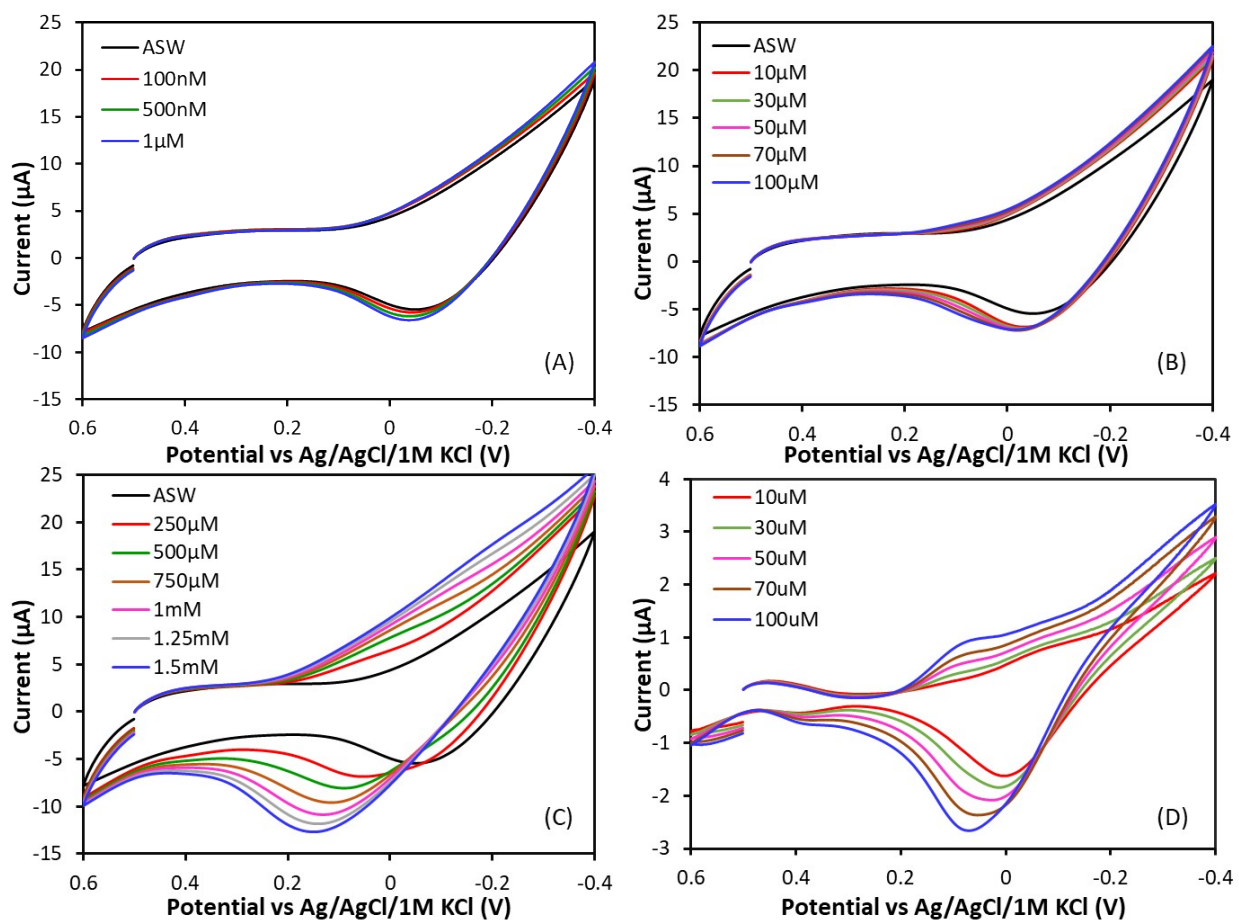
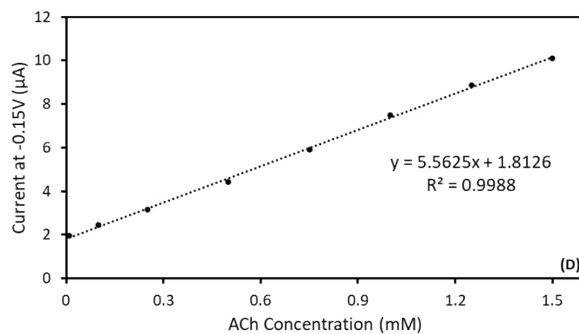
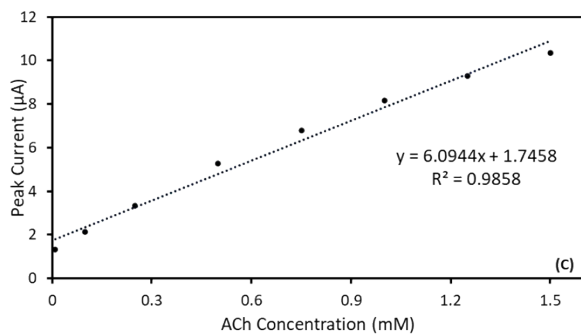
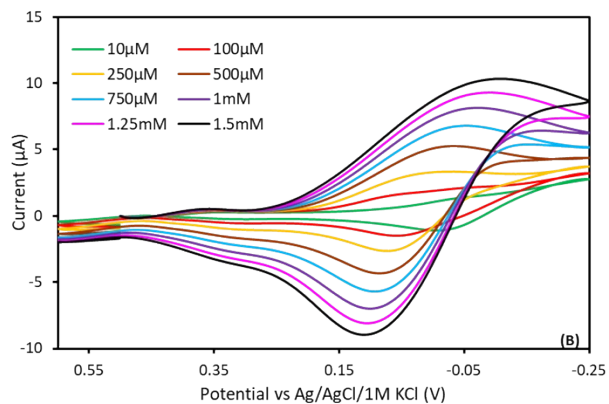
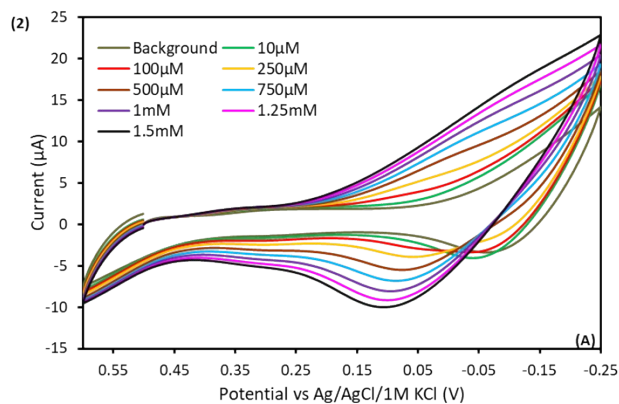
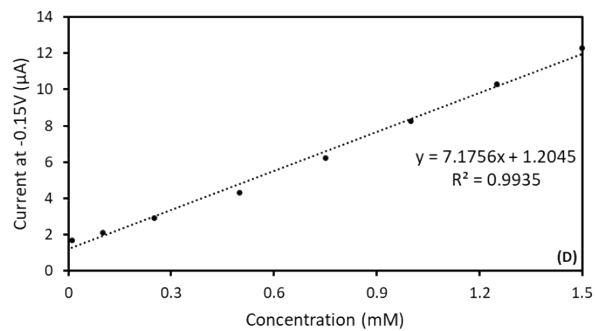
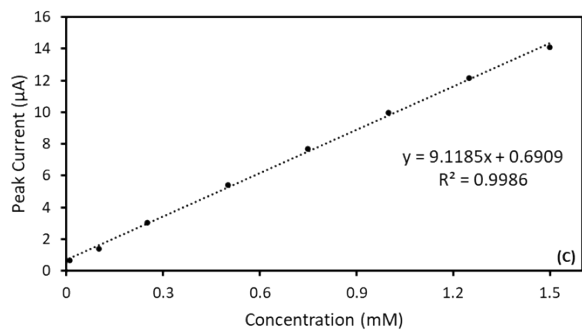
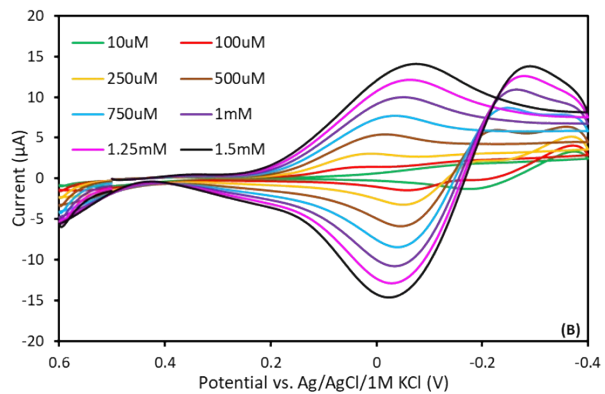
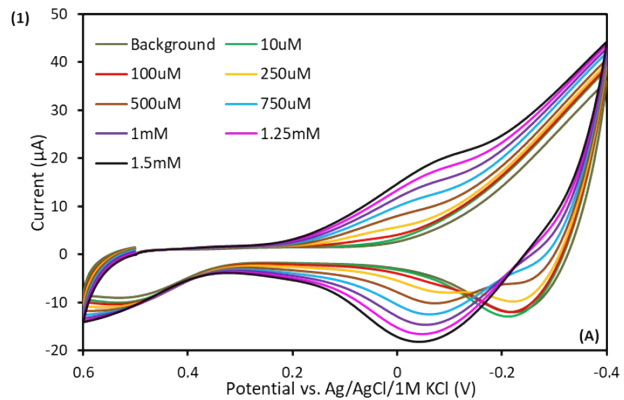


Figure S7. CVs illustrating ACh detection with expanded concentration ranges included. (A) CVs for background (ASW), and 100 nM, 500 nM and 1 μM ACh added, respectively. (B) CVs for 10 μM to 100 μM ACh solution, there is a slight increase in current between 0.2 V to 0 V. (C) CVs for 250 μM to 1.5 mM ACh solution, there is an obvious increase in current between 0.2 V to 0 V. (D) Background subtracted CVs for 10 μM to 100 μM ACh solution, there is an oxidation peak between 0.2 V to 0 V.



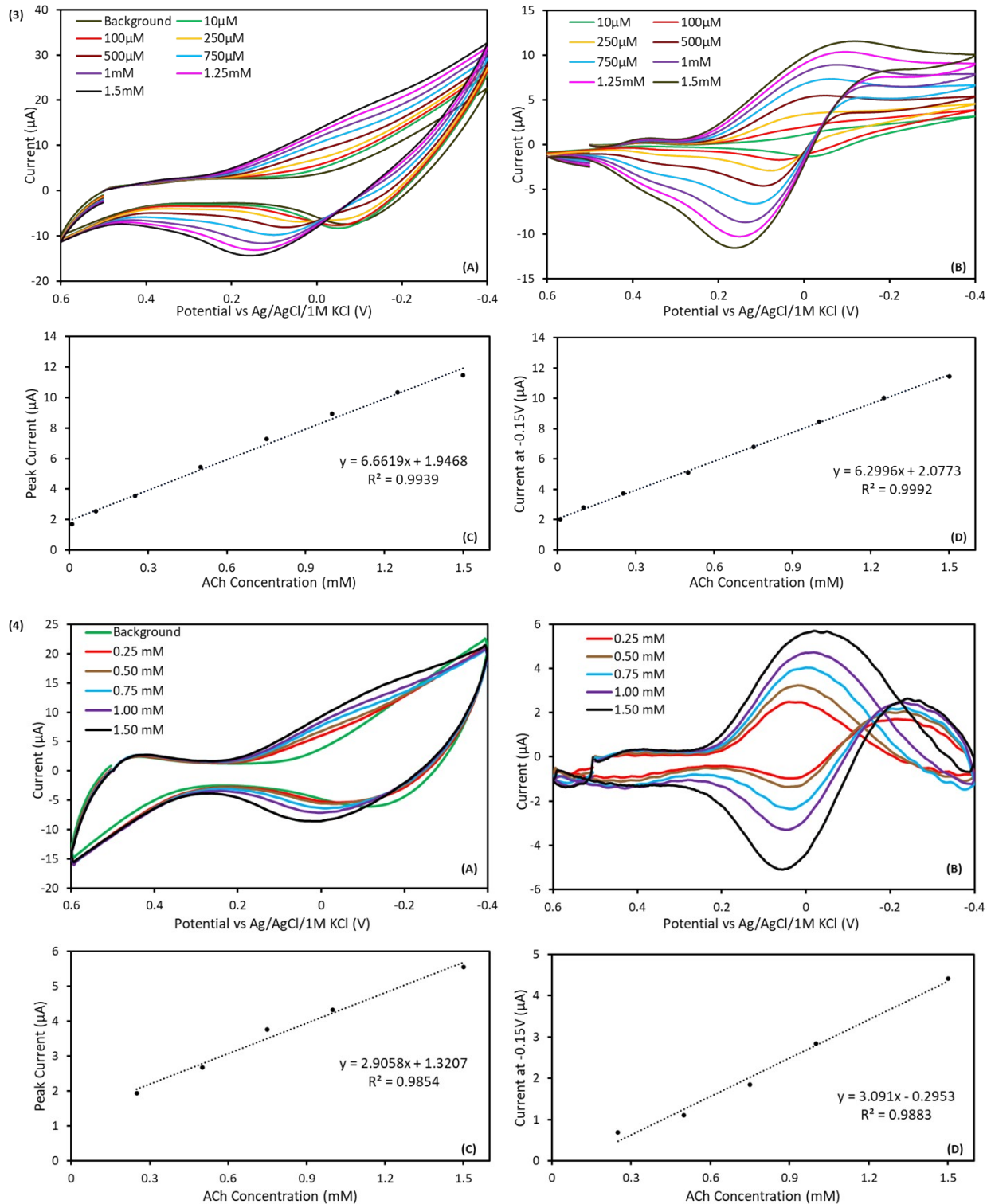


Figure S8. Additional CVs and calibration curves for amperometric ion-selective electrode showing consistency of the results between different researchers, different glassy carbon electrodes, and different supporting electrolytes. (1) Researcher 1 with glassy carbon electrode 1 and TBAPF₆ as the supporting electrolyte. (2) and (3) are repetitive runs by researcher 2 with glassy carbon electrode 3 and TBAPF₆ as the supporting electrolyte. (4) Researcher 3 with TDDATFAB as the supporting electrolyte. For each

figure: (A) Raw CVs, (B) background-subtracted CVs, (C) calibration curve at peak current, and (D) calibration curve at diffusion limiting region. The calibration curves showed great linearity between current and ACh concentration irrespective of the differences between electrodes and researchers. These results show high reproducibility for our newly developed amperometry ion-selective ACh electrode.

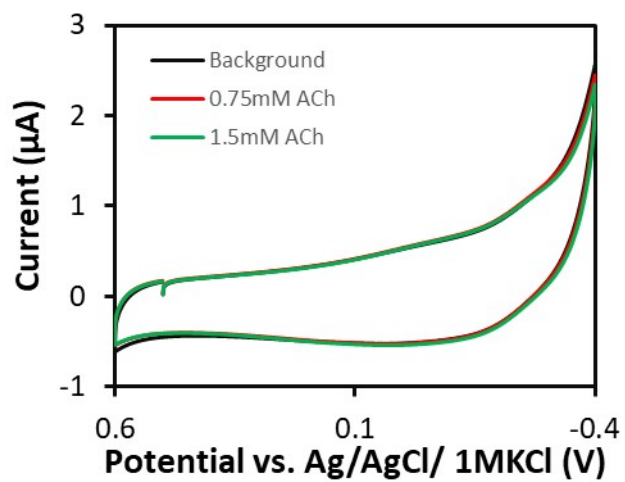


Figure S9. CVs on bare carbon electrode before modification. The voltammograms after adding ACh overlaid with that of the background, suggesting that there is no detection of ACh on bare carbon electrode.

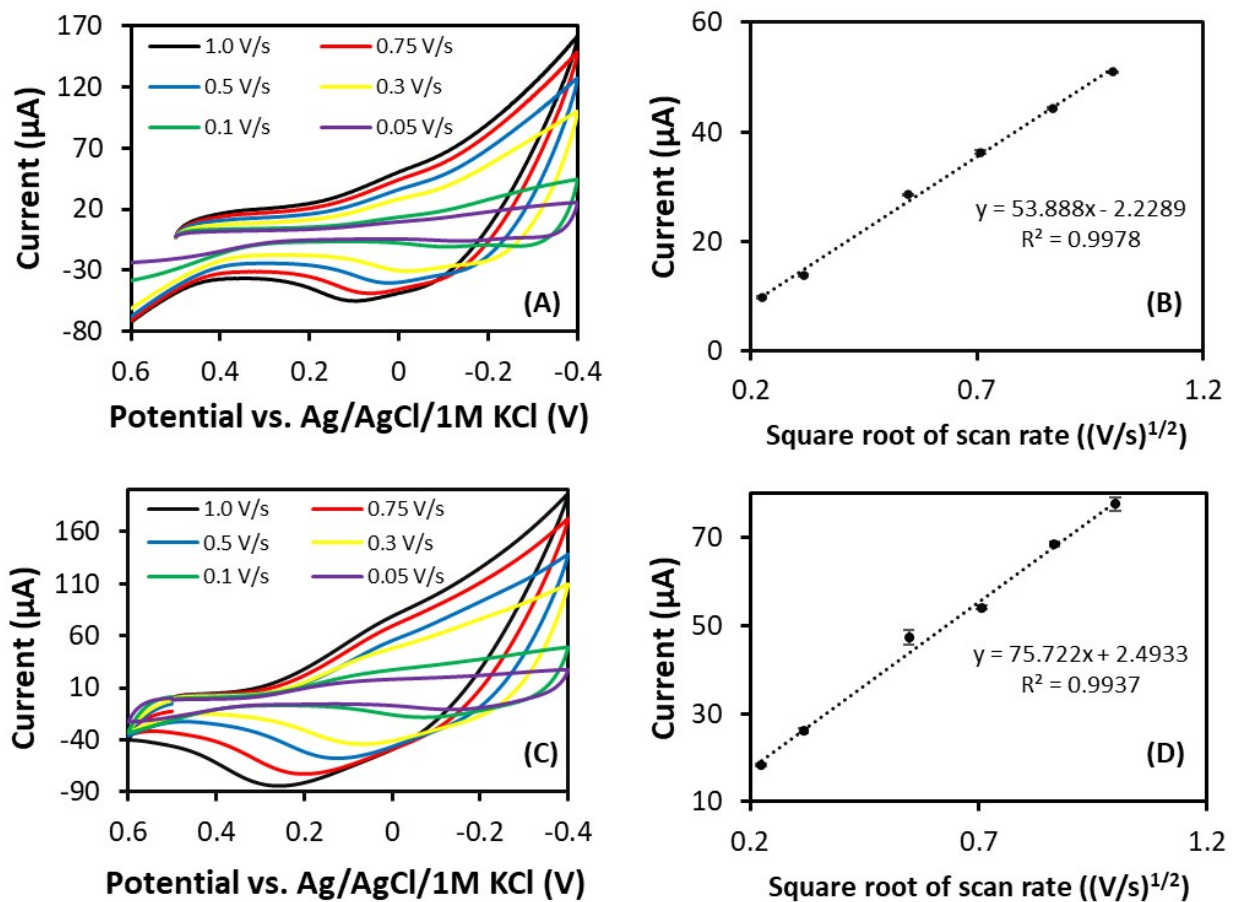


Figure S10. CVs with varying scan rates. (A) CVs for 0.5 mM ACh with different scan rates. (B) Plot of current versus the square root of scan rate. ACh concentration is 0.5mM. (C) CVs for 1.5 mM ACh with different scan rates. (D) Plot of current versus the square root of scan rate. ACh concentration is 1.5 mM. The linear relationship between current and the square root of scan rate suggests the detection of ACh occurs through a solution diffusion process.

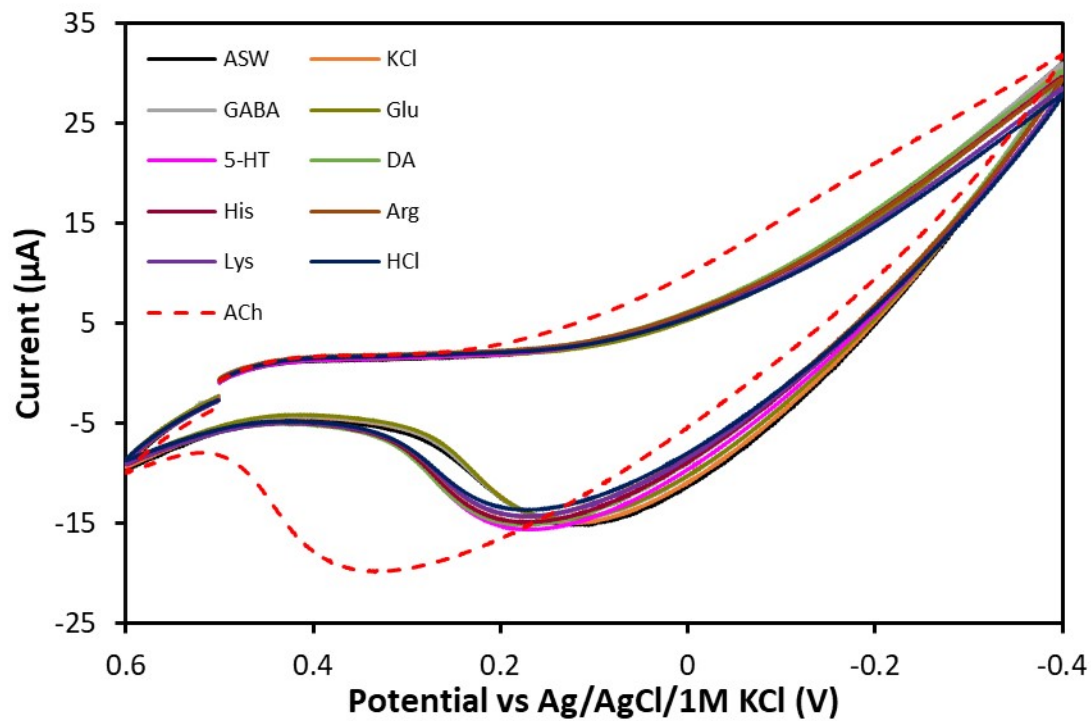


Figure S11. Selectivity study using CVs. CVs after adding interfering species overlapped with that of the background and a significant increase in current was observed after adding ACh, suggesting the selective detection towards ACh against the interfering species. The three repetitive runs for each interfering species showed overlapping responses. Error bar in Figure 5 is the standard deviation ($n=3$).

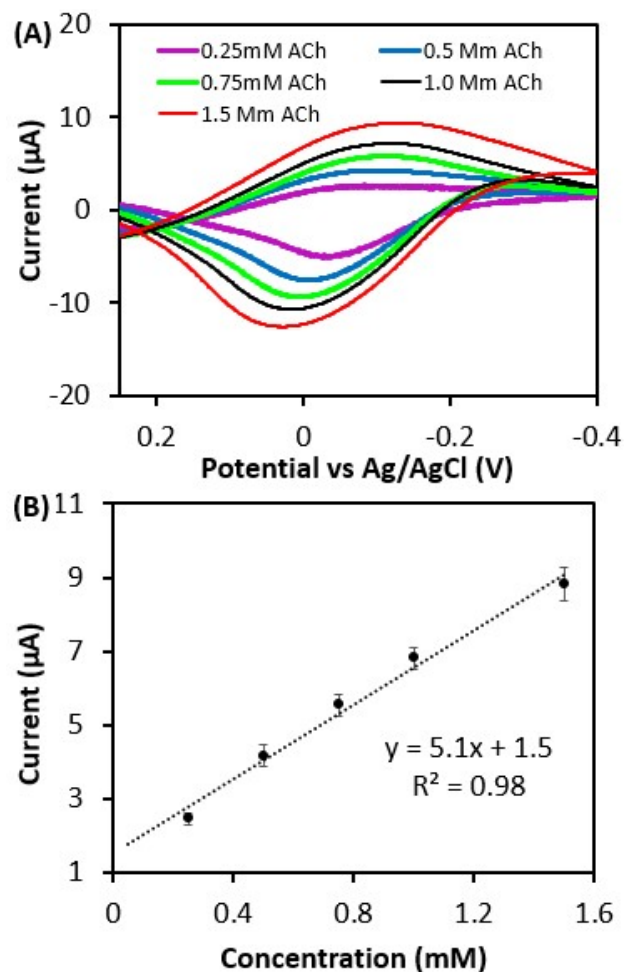


Figure S12. Stability of amperometric PVC / PEDOT-modified glassy carbon electrode for the detection of ACh tested 2 months after the fabrication of the acetylcholine (ACh) sensor. (A) Background-subtracted CVs corresponding to ACh detection at varying concentrations. (B) The calibration curve for ACh detection with the current measured at the diffusion-limited region, i.e., 80 mV passing the peak potential.

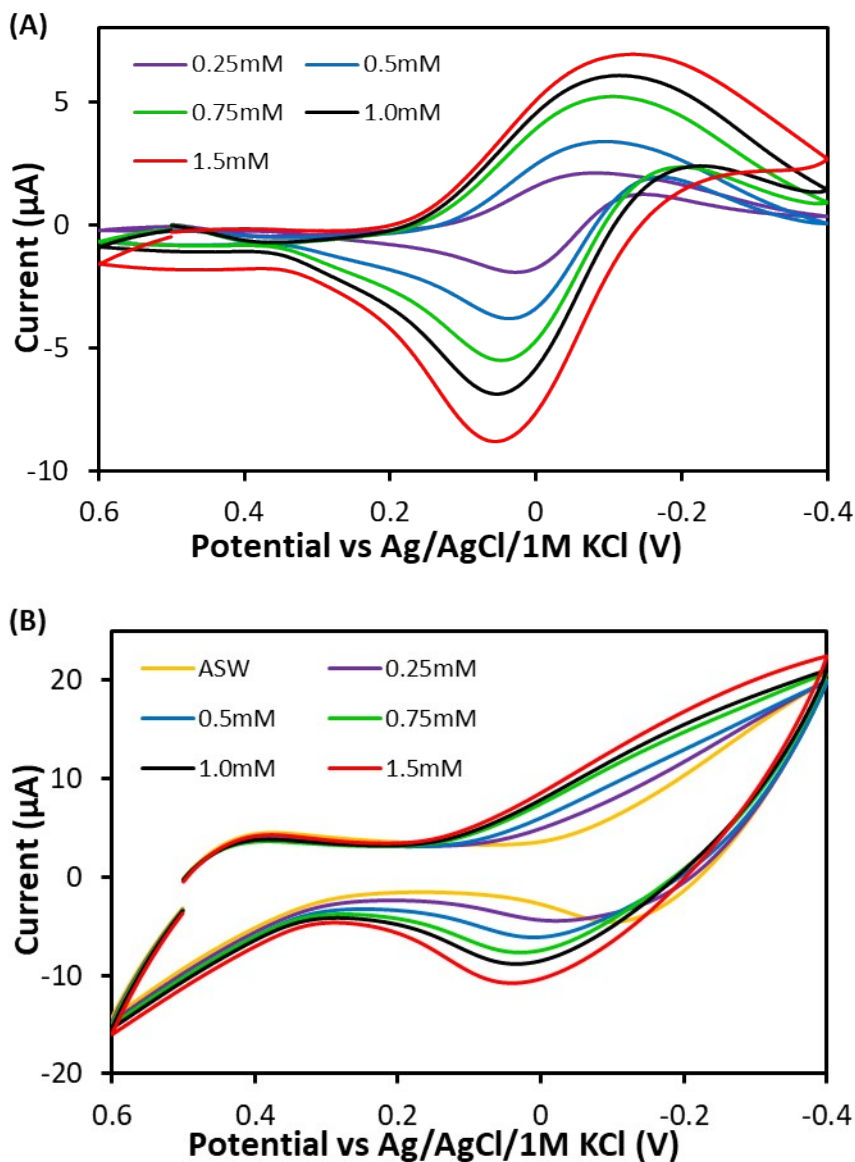


Figure S13. Stability test results. The electrode was stored for two months then used to test ACh detection response. (A) Background-subtracted CVs for full potential range. (B) Original CVs before background subtraction. We are still able to see clear detection for ACh, which means the electrode is capable of ACh detection after 2-month storage, showing a great stability of our electrode.

References

- 1 Nasrazadani, S. and Hassani, S. (2016). Modern analytical techniques in failure analysis of aerospace, chemical, and oil and gas industries. In *Handbook of materials failure analysis : with case studies from the oil and gas industry* pp. 39–54. Elsevier,.
- 2 Wolfgang, W. J. (2016). Chemical analysis techniques for failure analysis. In *Handbook of materials failure analysis with case studies from the aerospace and automotive industries* pp. 279–307. Butterworth-Heinemann,.